# ChemComm

Accepted Manuscript


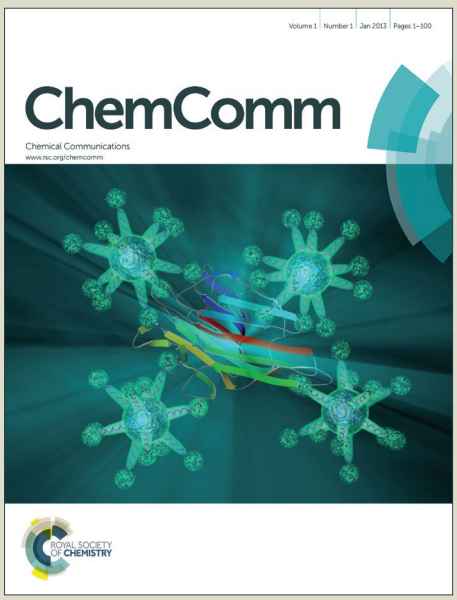





ROYAL SOCIETY OF CHEMISTRY

www.rsc.org/chemcomm

Cite this: DOI: 10.1039/c0xx00000x

www.rsc.org/xxxxxx

COMMUNICATION

# Hierarchical Nanostructures of γ-TaON Flower for Enhanced Visible Light Photocatalytic Activities

**Zheng Wang*, Keng Xie, Lei Zhao and Bangsheng Zhang**

***Received (in XXX, XXX) Xth XXXXXXXXX 20XX, Accepted Xth XXXXXXXXX 20XX***

**DOI: 10.1039/b000000x**

**Hierarchical nanostructures of single phase γ-TaON flower have been successfully synthesized by a simple wet-chemical route in addition with subsequent thermal nitridation. These flower-like particles exhibit an obvious improvement in visible-light-driven photocatalytic activity.**

Recently, the development of clean chemical energy produced by solar energy conversion has attracted great attention, due to the global energy crisis and demand for environmental protection.[1-3] Among all the possible means to make use of solar energy, solar water splitting is remarkable since it can accomplish the conversion of solar energy into chemical energy straightforward.[4-6] It is widely recognized that photocatalytic properties and performances of nanomaterial are highly related to their controlled morphologies and structures. Three-dimensional hierarchically nanostructured materials have the apparent advantages of enhancing light absorption, promoting the transport and separation of photoexcited charge carriers, and providing abundant exposed surface reaction sites, which are crucial for obtaining high solar energy conversion efficiency. [7-11]

Tantalum oxynitrides, among various potential semiconductor photocatalysts, have small band gaps to respond to visible-light, and they can realize overall solar water splitting with the proper positions of conduction band minimum and valence band maximum.[12-17] For instance, the preparation of one-dimensional TaON nanotube arrays were reported by Banerjee et al.[18] TaON nanotubes showed efficient visible light driven photocatalysts for photoelectrochemical generation of hydrogen from water. Macroporous TaON was synthesized by Tsang et al.[19] using PS spheres as the template, which exhibited the enhanced photocatalytic properties. Obviously, the properties of hierarchical tantalum oxynitrides are attracting more and more attention. In the previous work, our group has confirmed that the photocatalysis property of hollow urchin-like γ-TaON particle was significantly different from that of smooth particle. In addition, we found that the γ phase TaON showed the higher activity than common β phase TaON.[20] In this article, we take special note of the formation mechanism of the flower-like hierarchical γ-TaON (denoted as TNF) sphere and study its photocatalytic properties.

The three-dimensional (3D) TNF photscatalyst is synthesized by a simple wet-chemical route in addition with subsequent thermal nitridation. In a typical synthesis procedure, at first, stoichiometric tantalum powder (black-colour) was added to a certain amount of hydrofluoric acid and hydrogen peroxide aqueous solution, which was then hydrothermally treated at 240 °C for 6 h. Secondly, the γ-TaON samples were prepared by nitridation via the controllable thermal time.

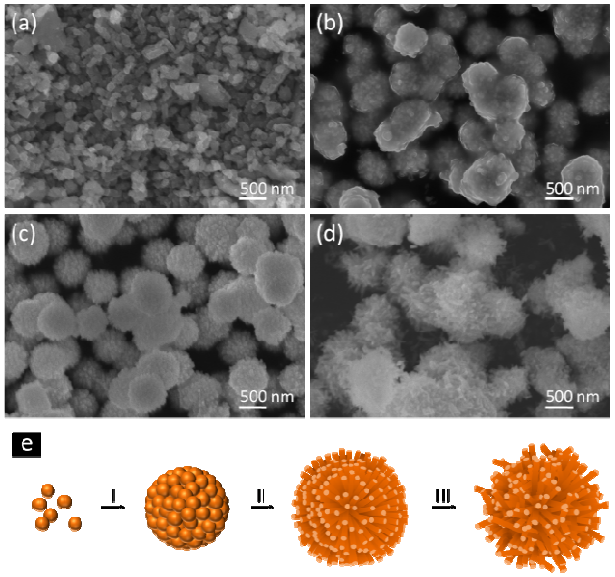


**Fig. 1** SEM images of as-prepared TOF hierarchical nanostructures with different hydrothermal times: (a) TOF1, (b) TOF3, (c) TOF6, and (d) TOF12. (e) Schematic illustration of the formation process of TOF hierarchical nanostructures.

To understand the growth mechanism of the $Ta_2O_5$ flower-like architectures (denoted as TOF), the influences of hydrothermal time on the structures and morphologies of the products have been investigated (Fig 1a-d). It is clearly observed that the time has great effect on the morphology of the products. After 3 hour hydrothermal process, the non-hierarchical nanospheres are formed (Fig. 1b) and the morphology is different from the raw material. When the hydrothermal time is increased to 6 hours, uniform and flower-like 3D hierarchical nanostructures, which consist of well-organized independent nanoneedles with the diameter of 5 nm and the length of 200~400 nm, are obtained (Fig. 1c and Fig. S2c). The HRTEM image of the tip of the

nanoneedles in Fig. S2e evidences the single crystalline nature of the nanoneedles. The distance between the adjacent lattice fringes 0.388 nm can be assigned to the interplanar distance of TOF nanostructures (001) in combination of the XRD result (Fig S1). After 12 hours hydrothermal process, the flower-like nanostructures grow to irregularly regimented particles. According to the time-dependent evolution of morphology, the growth process as depicted in Fig. 1e. At the initial stage of reaction, Ta powders are quickly etched to $H_2TaF_7$ by HF and then a large number of $Ta_2O_5$ nanoparticles are firstly hydrolyzed.[21, 22] After that, the nanoparticles aggregate into non-hierarchical nanospheres (Fig. 1e (I)). This process is called nucleation and self-assembly.[23] As the reaction time increases, the small nanocrytal and amorphous $Ta_2O_5$ nanoparticles are dissolved and recrystallized to gradually form $Ta_2O_5$ nanoneedles on the surface of nanospheres (Fig. 1e (II)) in order to maintain a more stable thermodynamics state. This process is called dissolution and recrystallization.[24] After excess growth, the nanoneedles aggregate and become longer and disorder as shown in Fig. 1e (III).

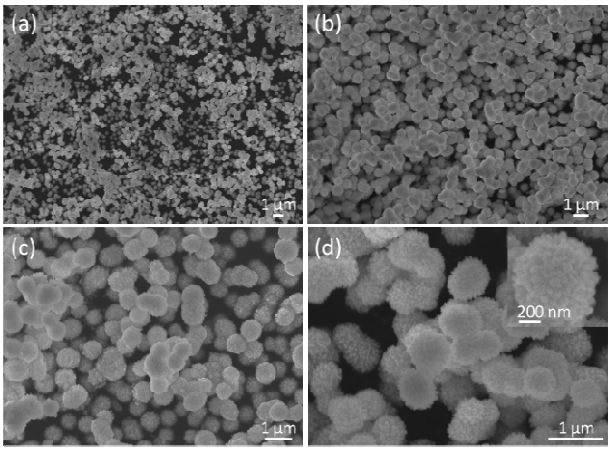


**Fig. 2** SEM images of as-prepared γ-TaON flowers under different magnification.

γ-TaON flower with hierarchical nanostructures were synthesized via subsequent thermal nitridation. The formation of the as-prepared TNF was demonstrated in Fig.2 and Fig. S2. It is found that the TNF spheres are uniform and high yield with diameter about 600~800 nm. The flower-like hierarchical nanostructures consist of well-organized independent nanoneedles with the length of 100~200 nm and the diameter about 10~20 nm (Fig. S2 d and f). The crystal structures of TNF spheres and pristine β-TaON were analysed by XRD patterns shown in Fig. 3a. The diffraction peaks of TNF match those of the crystalline monoclinicphase of γ-TaON (ICCD card no. 01-076-3258).[25] Full nitrogen sorption isotherms of the hierarchical nanostructures TNF were measured to gain information about the specific surface area, as shown in Fig. 3b. The specific surface area was calculated to be 51.3 $m^2 g^{-1}$ by the BET equation and the corresponding Barrett-Joyner-Halenda (BJH) analyses (the inset in Fig. 3b) exhibit that most of the pores fall into the size range from 10 to 80 nm. The high surface area structure of the hierarchical TNF particles provides the possibility for the efficient diffusion and transportation of electrons and holes in photochemical reactions, which will lead to the enhanced photocatalytic performance of the TNF materials.

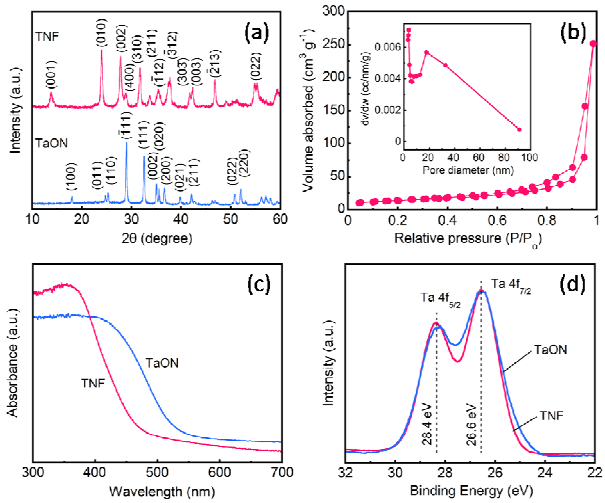


**Fig. 3** (a) XRD patterns of as-prepared TNF; (b) Nitrogen adsorption-desorption isotherm of the TNF and the corresponding pore size distribution obtained from the desorption curve; (c) UV-vis absorption spectra of TNF; (d) XPS spectra of Ta 4f for as prepared TNF.

UV-vis diffuse reflectance spectra of the TNF are shown in Fig. 3c. Compared with normal β-TaON, the TNF samples exhibit a significant increase in photoabsorption over the range of the spectrum and a red shift of the absorption edge to shorter wavelength. The direct band gaps of the TNF sample was determined according to the Kubelka-Munk method and its value is estimated at 2.75 eV, which is in good agreement with the previous work.[10, 20] The chemical states of as-prepared TNF architectures shown in Fig. 3d were carefully checked by X-ray photoelectron spectroscopy (XPS). The high-resolution XPS spectra show the Ta 4f7/2 line at 26.6 eV and 4f5/2 line at 28.4 eV in TNF sample indicating that tantalum is in the formal 5+ state, which are consistent with date of β-TaON particles.

The photocatalytic $H_2$ production activity on TNF photocatalysts with different hydrothermal time and with different morphology (denoted as TNF1, TNF3, TNF6, and TNF12 as shown in Table 1) was evaluated under irradiation of a xenon arc lamp, together with that on normal β-TaON for a comparison (Fig. 4). A trend in the photocatalytic activity has been observed in the following order: TNF6 > TNF12 > TNF3 > TNF1. The photocatalytic activity of the TNF architectures upon visible light irradiation increased with the hydrothermal time except for sample TNF12. High rate, more than 100 μmol $h^{-1}$, for $H_2$ evolution for the TNF hierarchical nanostructures were achieved while the hydrogen yield is only about 50 μmol $h^{-1}$ with the use of the pristine TaON. Among these samples, TNF6 samples exhibited a gradually enhanced photoactivity for water splitting as compared to other samples and demonstrated a high rate of hydrogen production at 329.1 μmol $h^{-1}$ with an apparent quantum efficiency of 7.5% under 420 nm light, which almost 7 times higher than that of common TaON. This high $H_2$ production photoactivity can be ascribed to the hierarchical

nanoneedles assembled structures. The space of serried nanoneedles is beneficial to multiple reflections of trapped incident light, thus enhancing light harvesting and increasing the quantities of photogenerated electrons and holes that participate in photocatalytic reactions, which was also observed in other works that the flower-like could much enhanced the photocatalytic activity.[26, 27] The stability tests were investigated by carrying out recycling reactions for 30 h for the hydrogen evolution over the TNF samples and the results are shown in Fig. S3. No obvious decrease in catalytic activity was observed in the recycling reactions, demonstrating the good stability of TNF. Furthermore, combined with previous and following XRD pattern of samples, no second phase was observed after photocatalytic reaction and the morphology is also not changed after reaction (Fig. S4). Thus, all abovementioned results indicate that the hierarchical TNF flower-like structures are promising candidates as visible-light photocatalysts.

**Table 1.** Physicochemical properties of the TNF samples[a]

| samples | average pore size (nm) | $S_{BET}$ ($m^2$ $g^{-1}$) | $H_2$ production rate (μmol $h^{-1}$) | QE (%) |
|---|---|---|---|---|
| TNF1 | 20.5 | 5.3 | 98.2 | 1.4 |
| TNF3 | 17.4 | 19.5 | 184.8 | 3.1 |
| TNF6 | 16.1 | 51.3 | 329.1 | 7.5 |
| TNF12 | 15.2 | 50.4 | 301.2 | 7.0 |
| TaON | - | 4.5 | 53.2 | 1.2 |

[a]All composite photocatalyst samples contain 0.1 wt.% of cocatalyst. Reaction conditions: catalyst, 0.3 g; reactant solution, 10:1 water: methanol solution, 200 mL; light source, xenon lamp (300 W) with cut-off filter (λ > 420 nm); reaction vessel, top-irradiation type; 1 h irradiation.

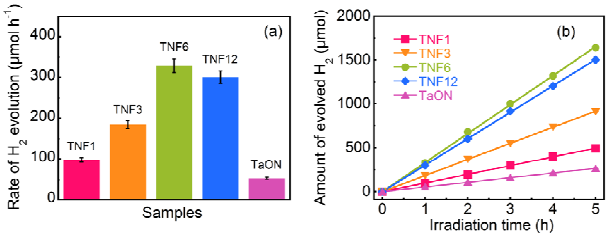


**Fig. 4** $H_2$ production rates of the TNF particles; (b) Comparison of the photocatalytic hydrogen production activities of different samples under the illumination with the same lighting source.

In summary, a high efficiency of the photocatalytic $H_2$ production from water splitting under visible light irradiation has been achieved over the flower-like single phase γ-TaON hierarchical nanostructures photocatalyst synthesized by a simple wet-chemical route without using any template or surfactant. The obtained samples were characterized by X-ray diffraction, electron microscopy, X-ray photoelectron spectra, UV-vis diffuse reflectance spectra and BET surface area. Based on observations of the factors that influence architecture formation, a possible growth mechanism is proposed to explain the transformation of nanoparticles to nanoflowers via a self-assembly mechanism followed by dissolution and recrystallization. The three dimensional flower-like γ-TaON architectures due to the synergistic effect of gamma phase crystal structure and large specific surface area exhibited an outstanding activity toward the water-splitting for hydrogen production as high as 329.1 μmol $h^{-1}$ under visible light irradiation, which was about 7 times higher photocatalytic activities than conventional TaON particles. Hence, similar concepts of this work can be used in other solar photovoltaic devices such as solar cells, photodegradation, and photo-conversion of carbon dioxide.

This work was supported by National Science Foundation of China (No. 51402017 and 51404026).

## Notes and references

*Department of Metallurgy, Beijing General Research Institute of Mining and Metallurgy, Beijing 100070, P. R. China. Fax: +86-10-59069564; Tel: +86-10-59069564; E-mail: wz_andrew@163.com*

† Electronic Supplementary Information (ESI) available: Experimental details, XRD pattern, TEM, etc. See DOI: 10.1039/b000000x/

1 M. R. Hoffmann, S. T. Martin, W. Choi and D. W. Bahnemann, *Chemical reviews*, 1995, **95**, 69-96.

2 A. J. Esswein and D. G. Nocera, *Chemical reviews*, 2007, **107**, 4022-4047.

3 M. G. Walter, E. L. Warren, J. R. McKone, S. W. Boettcher, Q. Mi, E. A. Santori and N. S. Lewis, *Chemical reviews*, 2010, **110**, 6446-6473.

4 W. Lubitz and W. Tumas, *Chemical reviews*, 2007, **107**, 3900-3903.

5 X. Chen, S. Shen, L. Guo and S. S. Mao, *Chemical Reviews (Washington, DC, United States)*, 2010, **110**, 6503-6570.

6 Q. Zhang, E. Uchaker, S. L. Candelaria and G. Cao, *Chemical Society reviews*, 2013, **42**, 3127-3171.

7 H. M. Chen, C. K. Chen, R.-S. Liu, L. Zhang, J. Zhang and D. P. Wilkinson, *Chemical Society reviews*, 2012, **41**, 5654-5671.

8 J. Zhu and M. Zäch, *Current Opinion in Colloid & Interface Science*, 2009, **14**, 260-269.

9 Z. Wang, J. Hou, C. Yang, S. Jiao, K. Huang and H. Zhu, *Physical Chemistry Chemical Physics*, 2013, **15**, 3249-3255.

10 Z. Wang, J. Hou, C. Yang, S. Jiao and H. Zhu, *Chemical Communications*, 2014, **50**, 1731-1734.

11 J. Hou, C. Yang, Z. Wang, Q. Ji, Y. Li, G. Huang, S. Jiao and H. Zhu, *Applied Catalysis B: Environmental*, 2013, **142**, 579-589.

12 G. Hitoki, T. Takata, J. N. Kondo, M. Hara, H. Kobayashi and K. Domen, *Chemical Communications*, 2002, 1698-1699.

13 M. Hara, T. Takata, J. N. Kondo and K. Domen, *Catalysis Today*, 2004, **90**, 313-317.

14 M. Hara, G. Hitoki, T. Takata, J. N. Kondo, H. Kobayashi and K. Domen, *Catalysis Today*, 2003, **78**, 555-560.

15 P. Zhang, J. Zhang and J. Gong, *Chemical Society reviews*, 2014, 4395-4422.

16 Z. Wang, J. Hou, S. Jiao, K. Huang and H. Zhu, *Journal of Materials Chemistry*, 2012, **22**, 21972-21978.

17 J. Hou, Z. Wang, W. Kan, S. Jiao, H. Zhu and R. Kumar, *Journal of Materials Chemistry*, 2012, **22**, 7291-7299.

18 S. Banerjee, S. K. Mohapatra and M. Misra, *Chemical Communications*, 2009, 7137-7139.

19 M. Y. Tsang, N. E. Pridmore, L. J. Gillie, Y. H. Chou, R. Brydson and R. E. Douthwaite, *Advanced Materials*, 2012, **24**, 3406-3409.

20 Z. Wang, J. Hou, C. Yang, S. Jiao, K. Huang and H. Zhu, *Energy & Environmental Science*, 2013, **6**, 2134-2144.

21 M. Gibalo, Analytical Chemistry of Niobium & Tantalum, ANN Arbor-Humphey Sci. Pubilishers, Inc., London, 1970.

22 J. Duan, W. Shi, L. Xu, G. Mou, Q. Xin and J. Guan, *Chemical Communications*, 2012, **48**, 7301-7303.

23 D. V. Bavykin, J. M. Friedrich and F. C. Walsh, *Advanced Materials*, 2006, **18**, 2807-2824.

24 J. Wu, S. Hayakawa, K. Tsuru and A. Osaka, *Scripta Materialia*, 2002, **46**, 101-106.

25 H. Wolff, T. Bredow, M. Lerch, H. Schilling, E. Irran, A. Stork and R. Dronskowski, *Journal of Physical Chemistry A*, 2007, **111**, 2745-2749.

26 S. Guo and S. Han, *Journal of Power Sources*, 2014, 9-13.

27 Q. Xiang, B. Cheng and J. Yu, *Applied Catalysis B: Environmental*, 2013, **138**, 299-303.